PHILOSOPHICAL TRANSACTIONS OF THE ROYAL SOCIETY A MATHEMATICAL, PHYSICAL & ENGINEERING SCIENCES

Stresses and Deformation at Grain Boundaries [and Discussion]

W. Beere and E. H. Rutter

Phil. Trans. R. Soc. Lond. A 1978 **288**, 177-196
doi: 10.1098/rsta.1978.0012

Phil. Trans. R. Soc. Lond. A. **288**, 177–196 (1978) [177]
Printed in Great Britain

Stresses and deformation at grain boundaries

By W. Beeré
Central Electricity Generating Board, Berkeley Nuclear Laboratories, Berkeley, Gloucestershire, U.K.

[Plates 1 and 2]

Grain boundary sliding is frequently observed during the creep of polycrystals and this can alter both the internal stresses and the creep rate. Sliding arises because the shear and normal forces acting on the grain boundaries can be relaxed by separate mechanisms at different rates. If sliding is easy the shear forces can in the limit tend to zero. The normal forces are then relaxed more slowly by plastic deformation inside the grain or by diffusion creep. While the former distorts the interior of the grain the latter does not. Several two dimensional models of the diffusion mechanism have appeared in which rigid slabs slide past each other. Diffusion plates out material on the boundaries and controls grain movement normal to the boundary. It is also possible to solve the 'rigid grain' situation in three dimensions when rapid diffusion at boundaries relaxes the normal forces. The shear process then controls the grain motion and it is necessary that the grains roll over each other.

1. Introduction

Grain boundary sliding is frequently observed in metals and ceramics deformed at elevated temperatures. Localized strains within the material can be highly inhomogeneous with extensive shear at the boundary planes. Sliding never occurs on its own in polycrystals, but has to be accompanied by other deformation mechanisms. The sliding and accommodating processes can conveniently be classified into three categories.

First, the grains can deform by diffusion creep, figure 1 (*a*). Material removed from one boundary is deposited at another thus moving adjacent grain centres normal to their common boundary.

Examination of the grain geometry shows that sliding must occur simultaneously to prevent gaps appearing at grain boundaries (Lifshitz 1963; Gibbs 1965; Stephens 1971; Gates 1975). The grain interior does not deform and all displacements of adjacent grain centres parallel to a common boundary have to take place by boundary sliding. Diffusion creep and grain boundary sliding are mutually accommodating. Usually the sliding process has a short relaxation time compared with diffusion across the grain. Thus the shear stresses on the boundaries necessary to cause sliding at a rate compatible with the diffusion process are vanishingly low (Raj & Ashby 1971).

A similar type of deformation can be envisaged again in which the interior of the grain does not deform, but in which boundary shear forces are large, figure 1 (*b*). An important feature of this type of deformation is grain rotation. Frictional forces developed on the boundary rotate the atomic lattice (Beeré 1976). Possible applications are in superplastic creep and diffusion creep near a threshold stress.

Lastly, at higher stresses dislocation creep in the grain interior becomes important, figure 1 (*c*).

Shear between grain centres takes place both by shear inside the grain and by boundary sliding (Bell & Langdon 1969; Crossman & Ashby 1975; Speight 1976).

Examples of all three categories are available. Figure 2, plate 1, is a scanning electron micrograph showing sliding offsets during the diffusion creep of hyperstoichiometric UO_2 (Reynolds, Burton & Speight 1975). The scratch lines produced during polishing of the originally flat surface show clear offsets at grain boundaries. The scratch lines remain straight in the grain interior indicating a negligible contribution from dislocation creep. Some grains have moved normal to the surface and a few grain boundaries have separated. The UO_2 was crept under

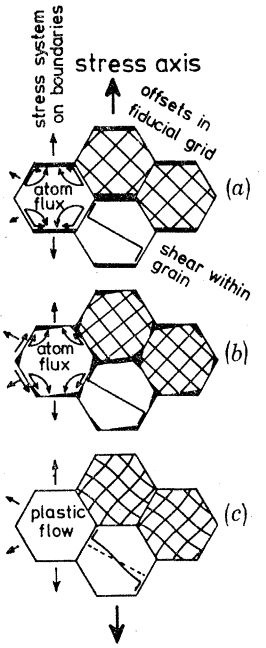

FIGURE 1. Three categories of grain boundary sliding: (*a*) diffusion creep (zero boundary shear stress); (*b*) rigid grain creep (finite boundary shear stress); and (*c*) dislocation creep (with grain boundary sliding). Types (*a*) and (*b*) have rigid grain interiors while the grain interior deforms plastically in (*c*). Grain boundary shear forces are absent in (*a*) and can be fully relaxed in (*c*) but are present in (*b*).

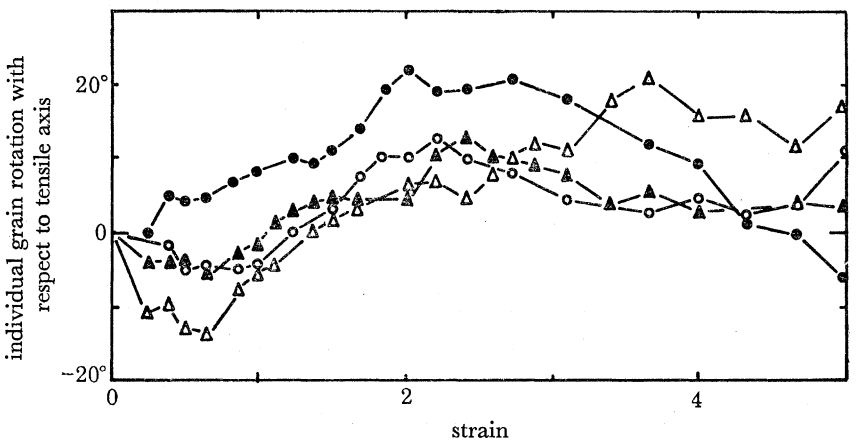

FIGURE 3. Grain rotations observed during creep of a Pb/Sn eutectic (Geckinli & Barrett 1976).

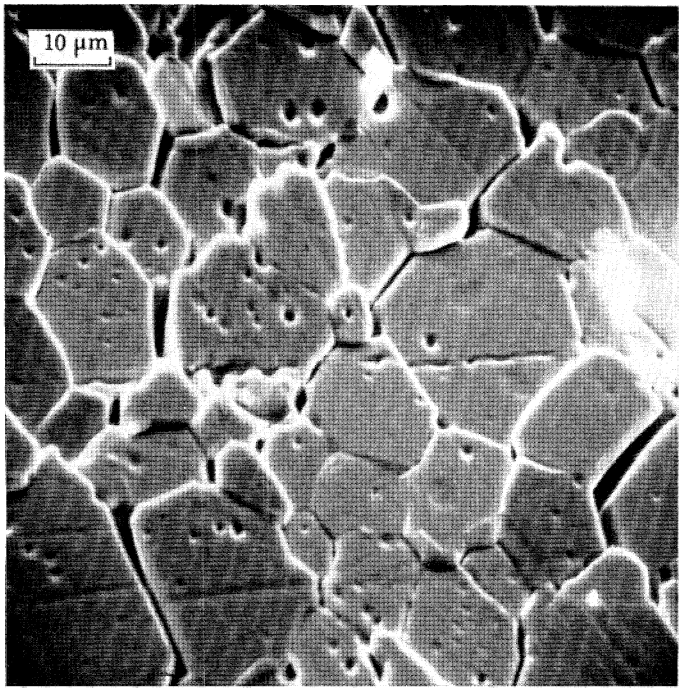

FIGURE 2. A scanning electron micrograph of UO_2. The initially flat polished surface shows ledges, sliding offsets of surface scratches and cracks resulting from grain boundary sliding during creep. (Reynolds *et al.* 1975.)

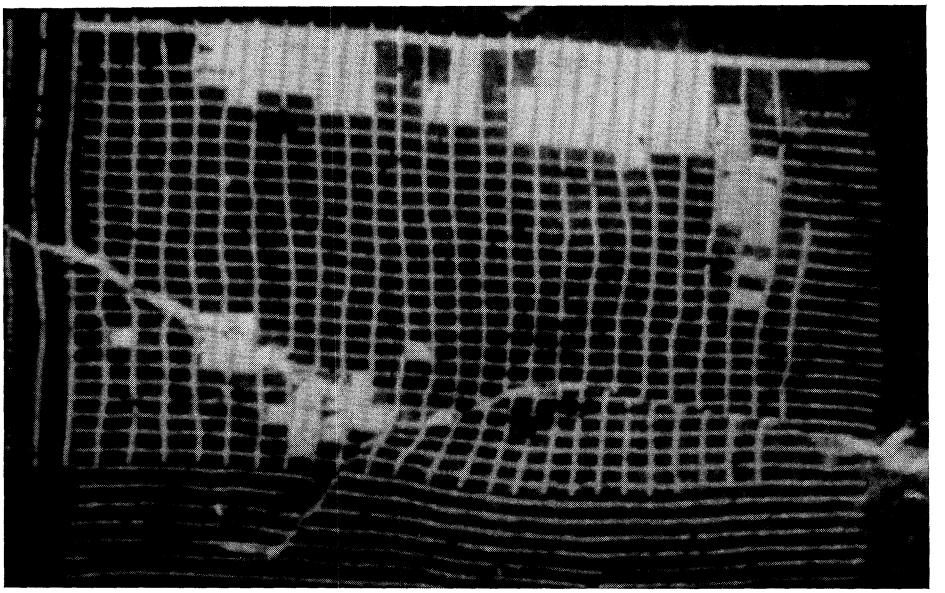

FIGURE 4. Deformation by grain boundary sliding and dislocation creep of an initially rectangular 8 μm grid on aluminium. (Pond *et al.* 1976.)

(*Facing p.* 178)

PHILOSOPHICAL TRANSACTIONS OF THE ROYAL SOCIETY A MATHEMATICAL, PHYSICAL & ENGINEERING SCIENCES

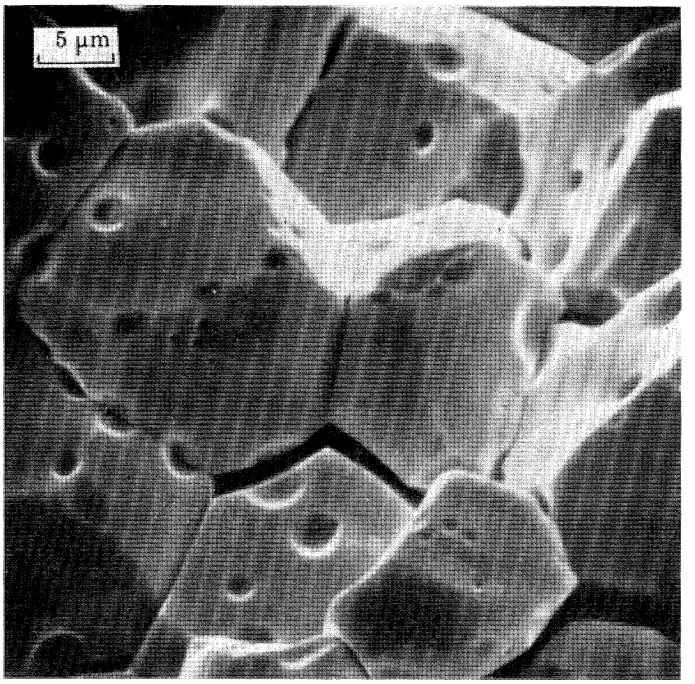

FIGURE 8. Cracks in a UO_2 compression specimen. The wedging action of adjacent grains coupled with grain boundary sliding produces tensile forces and cracking. (Reynolds *et al.* 1975.)

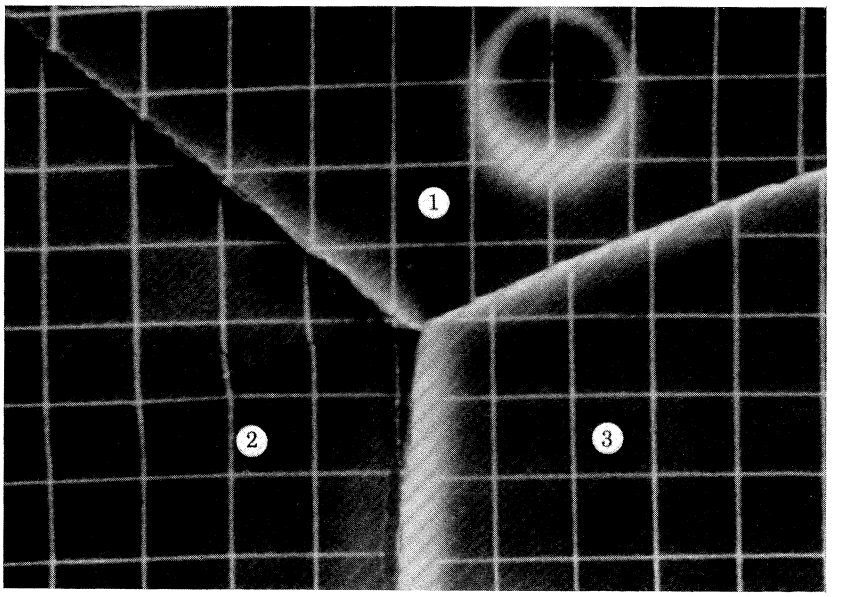

FIGURE 13. Grain boundary sliding in aluminium revealed by displacements in an initially rectangular 8μm grid. Sliding between grains 1 and 3 has created a slip band in grain 2. (Pond *et al.* 1976.)

PHILOSOPHICAL TRANSACTIONS OF THE ROYAL SOCIETY A MATHEMATICAL, PHYSICAL & ENGINEERING SCIENCES

compression, but relaxation of the shear stresses results in tensile forces developing across certain boundary orientations.

Significant grain rotation occurs during stage II superplastic creep. Figure 3 shows the angular variation of four grains in a lead tin eutectic (Geckinli & Barrett 1976). Quite large rates of rotation are observed although the angular variation seldom exceeds 30°.

Dislocation creep and grain boundary sliding are common to a very large number of systems. Figure 4, plate 1, shows a scanning electron micrograph of pure aluminium crept at high temperature *in situ* in the scanning electron microscope (Pond, Smith & Southerden 1976). The grid bars were originally a rectangular array spaced 8 μm apart before creep. After deformation the grid shows internal grain deformation and sliding along the three boundaries present.

Analysis of combined sliding and accommodating deformation is facilitated by knowledge of the boundary stresses and the possible sliding displacements. The two types of sliding with rigid grain interiors, figure 1 (*a*, *b*), are now examined in detail.

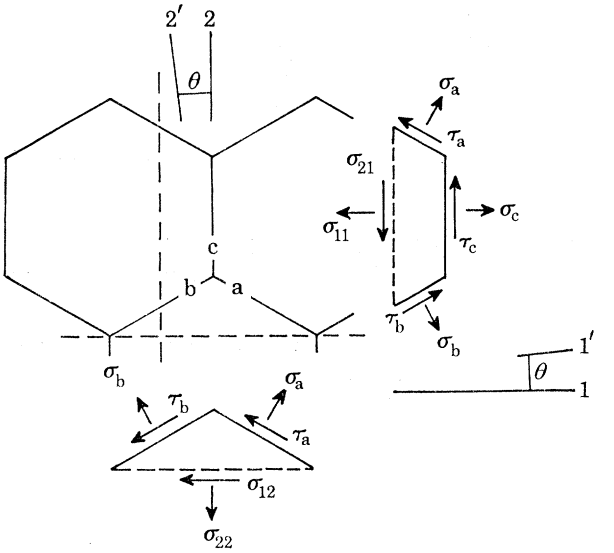

FIGURE 5. The stresses acting on idealized hexagonal grains and elements of grains.

2. STRESSES ACTING ACROSS GRAIN BOUNDARIES

The normal and shear stresses on a boundary in a homogeneous body behave as tensors and their value can be calculated simply from the boundary orientation. When the boundaries slide the body becomes inhomogeneous, the boundary stresses change and have to be recalculated taking the grain geometry into account. The complex morphology of real grains has not been treated, but typically a much simpler grain shape is substituted to ease calculations. Hexagonal grains are often chosen because they are the simplest shape in which three grain boundaries meet in a position of stable equilibrium. The stress system on the hexagon boundaries is calculated for an aggregate of many regular grains randomly orientated with respect to an applied uniaxial tensile stress. The same procedure could be followed for any superimposed system of stresses.

Figure 5 shows three grains of the aggregate. Each grain is assumed to be indistinguishable from its neighbours. Hence there are three types of boundary since for instance a vertical

boundary (figure 5) behaves identically to any other vertical boundary. The three boundary types are labelled a, b and c.

The stresses are calculated by removing elements of the grains and balancing forces. The stress distribution inside the grains is not known, but the internal stresses along the dashed lines (figure 5) repeat cyclically in each grain. Hence the average stress on the dashed face of one of the elements is the same as the average stress on the complete dashed line in the aggregate. Since the line passes completely through the aggregate the average stress must support the applied load and so its value is the same as the stress on a similarly orientated plane in a homogeneous

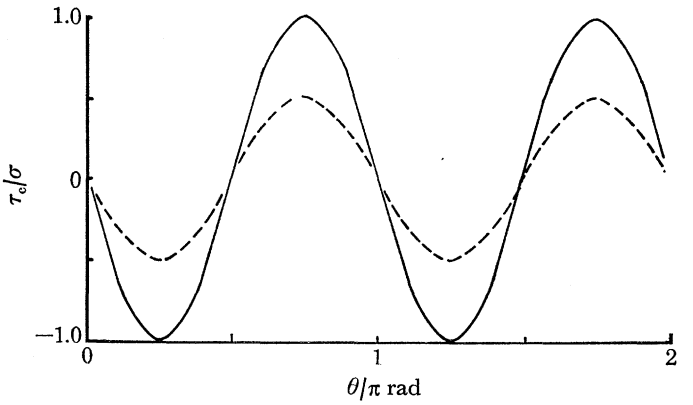

FIGURE 6. The shear force acting on a grain boundary of an idealized hexagonal grain for a homogeneous solid, broken line, and a grain with fully relaxed normal boundary forces.

body. Putting $\sigma_{11} = \sigma \cos^2\theta$, etc., where σ is the uniaxial stress and θ the angle between the stress axis and the 1 axis, the forces on the elements can be balanced vertically and horizontally giving

$$\tau_a + \tau_b + \tau_c = 0, \tag{1}$$

$$\sigma_a + \sigma_b + \sigma_c = \tfrac{3}{2}\sigma, \tag{2}$$

where τ_a and σ_a are the average shear and normal stresses on an 'a' boundary respectively and the subscripts b and c refer to the other boundaries.

The calculation can proceed further only if assumptions are made about the material properties. It is simplest to deal with complete relaxation of either the normal or the shear stresses on the boundary.

If for instance the normal stresses are relaxed they are everywhere equal because only an infinitesimal deviatoric stress is necessary. From equation (2) their value must be

$$\sigma_a = \sigma_b = \sigma_c = \tfrac{1}{2}\sigma.$$

The shear stress on a 'c' boundary is then (Beeré 1976)

$$\tau_c = 2\sigma \sin\theta \cos\theta, \tag{3}$$

which is exactly twice that for a homogeneous solid (figure 6). The stresses on the 'a' and 'b' boundaries can be found by adding multiples of $\frac{2}{3}\pi$ to θ. Conversely, if the shear stresses are relaxed, $\tau_a = \tau_b = \tau_c = 0$, then the normal stress on a 'c' boundary is

$$\sigma_c = \sigma(\tfrac{3}{2} - 2\sin^2\theta). \tag{4}$$

The normal stress is illustrated in figure 7 along with the stress in a homogeneous solid. Relaxing the shear stresses doubles the normal stresses about their mean value. During tensile creep compressive forces appear across certain boundaries. Likewise, if the external load is compressive tensile forces appear which can be large enough to cause fracture on the boundary. This is illustrated in figure 8, plate 2 (Reynolds *et al.* 1975), which shows a $UO_{2.2}$ specimen crept at 80 MPa and 1350 °C.

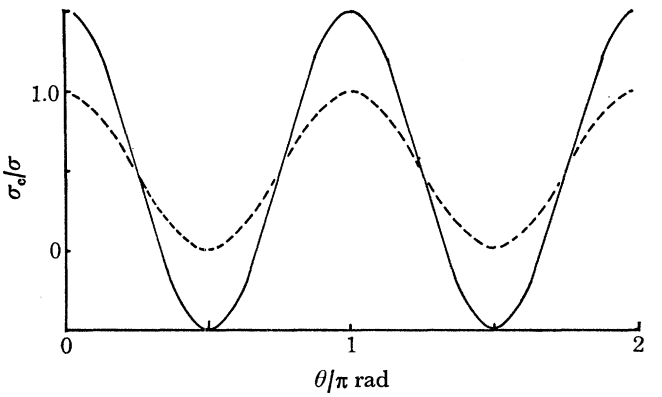

FIGURE 7. The normal force acting on a grain boundary of an idealized hexagonal grain for a homogeneous solid, broken line, and a grain with fully relaxed boundary shear forces.

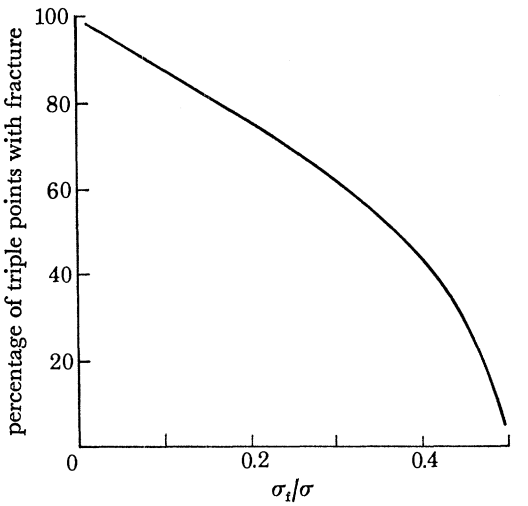

FIGURE 9. The percentage of triple points associated with a cracked boundary plotted against the ratio of average tensile fracture stress to applied compressive stress.

Significant fracture is expected to take place when the average tensile fracture stress is less than half the applied compressive stress. If it is assumed that fracture takes place when the average tensile stress exceeds a critical value σ_t, then assuming a random distribution of boundary orientations the percentage of boundaries fractured can be calculated from equation (4). The result is illustrated in figure 9. Thus if σ_t/σ is 0.45, the initial application of the external load causes about 30 % of triple points to be associated with a fractured boundary. An examination of the stress system near a fractured boundary reveals that the locality can no longer support an applied uniaxial stress. The grain can rapidly relax the local stress system by

grain boundary sliding redistributing part of its load onto unfractured grains. This causes more grains to fracture. If the fracture stress is sufficiently high this redistribution mechanism eventually stabilizes. Below a critical value of σ_f/σ the mechanism becomes unstable and the polycrystal suffers catastrophic fracture. This is best observed in doped ceramics in which the dopant segregates preferentially to the grain boundary reducing the fracture stress without significantly altering the creep properties of the grain. These materials are susceptible to catastrophic intergranular fracture during the application of large compressive stresses (Reynolds 1977).

TABLE 1

invariant	homogeneous solid	fully relaxed shear stresses
$\sigma_a+\sigma_b+\sigma_c$	$\frac{3}{2}\sigma$	$\frac{3}{2}\sigma$
$\sigma_a^2+\sigma_b^2+\sigma_c^2$	$\frac{9}{8}\sigma^2$	$\frac{9}{4}\sigma^2$
$\tau_a+\tau_b+\tau_c$	0	0
$\tau_a^2+\tau_b^2+\tau_c^2$	$\frac{3}{8}\sigma^2$	0

Equations (1) and (2) show that the sum of the normal and shear stresses are both invariant with respect to rotation of the applied stress. Other invariants are listed in table 1 with values when the boundary shear stresses are zero and for a homogeneous material. The 'invariants' can alter in value during boundary relaxation.

3. GRAIN MOTION

The previous section considered the stresses acting on grain boundaries. Next it is pertinent to ask how the boundary stresses plastically deform the grain. First, the geometry of the possible motions is considered followed by the rate of motion resulting from the material properties.

When the dominant deformation mechanism is diffusion creep the interiors of the grains do not deform. Material is transferred preferentially between boundaries usually by a vacancy mechanism. If again we treat a two dimensional array of hexagons, the hexagons behave as rigid slabs with some boundaries gaining material while others lose material. If the increase in distance between grain centres across an 'a' boundary is N_a and the sliding displacement is S_a then there are six separate movements (figure 10). These are not all independent. If gaps do not appear on the boundary during creep then analysis shows that the sum of the normal and sliding displacements are both zero, i.e.

$$N_a+N_b+N_c = 0, \tag{5}$$

$$S_a+S_b+S_c = 0, \tag{6}$$

where the subscripts refer to the boundary type. Equation (5) is simply a statement that the volume of material remains constant.

If the motion of one grain is indistinguishable from its neighbours then the motion between adjacent grain centres is identical to the bulk motion of the aggregate. When the aggregate deforms uniaxially by a strain ϵ the strain in the coordinate system of the grain centres, ϵ_{ij}, is given by the equation:

$$\epsilon = \epsilon_{11}\cos^2\theta+\epsilon_{22}\sin^2\theta+(\epsilon_{12}+\epsilon_{21})\sin\theta\cos\theta. \tag{7}$$

The strain between grain centres, ϵ_{ij}, can also be written in terms of the boundary displacements. Substitution into equation (7) gives the desired relation between the aggregate strain and the normal and sliding boundary displacements.

$$\epsilon d = -(N_a + N_b)\,(2\cos^2\theta - 1) + \frac{1}{\sqrt{3}}(N_a - N_b)\,2\sin\theta\cos\theta \tag{8}$$

$$= \frac{1}{\sqrt{3}}(S_a - S_b)\,(2\cos^2\theta - 1) + \frac{1}{\sqrt{3}}(S_a + S_b - 2S_c)\,2\sin\theta\cos\theta, \tag{9}$$

where d is the hexagon diameter.

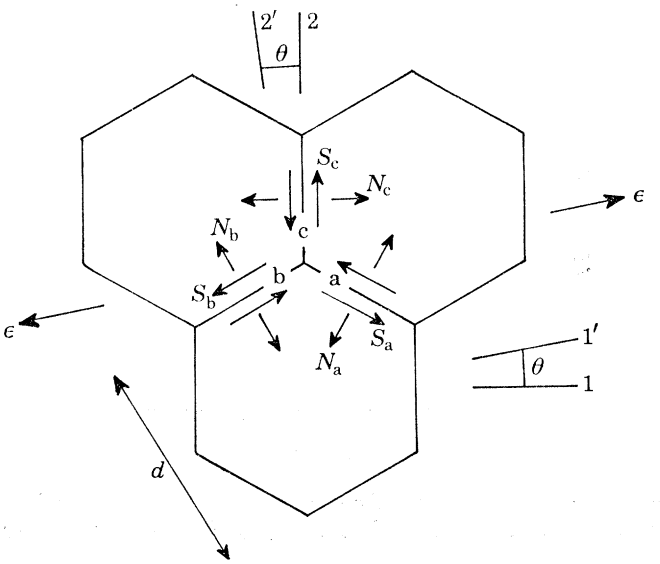

FIGURE 10. The three sliding and three normal displacements of adjacent grains at a triple point.

The bulk specimen strain can be defined completely in terms of the normal displacements or the sliding displacements. Thus, if diffusion changes the grain centre distances resulting in creep, sliding must also take place and both types of displacement are mutually accommodating.

4. DIFFUSION CREEP

The equilibrium concentration of vacancies adjacent to a grain boundary depends on the normal stress acting on the boundary. A difference in vacancy concentration between boundaries sets up a vacancy flux. If we consider an 'a' boundary the rate of separation $\dot{N}_a$ is given by

$$\dot{N}_a = \text{const}\; D\Omega(\sigma_a - \tfrac{1}{2}\sigma_b - \tfrac{1}{2}\sigma_c)/kTd, \tag{10}$$

where D is the volume self-diffusion coefficient, Ω the atomic volume, k Boltzmann's constant and T absolute temperature. The bracketed term takes account of the flux between both 'a' and 'b' and 'a' and 'c' boundaries. A detailed calculation gives the constant a value $3^{\frac{3}{2}}\pi^3/16$ (Beeré 1976).

When diffusion creep is the rate controlling mechanism the boundary shear forces are considered to be vanishingly small and the normal stresses will be given from the previous calculation. From equations (4), (8) and (10) the creep rate is

$$\dot{\epsilon} = 15D\sigma\Omega/kTd^2, \tag{11}$$

which is seen to be independent of orientation of the applied stress.

This equation has been derived previously by a number of workers (Gibbs 1965; Raj & Ashby 1971; Herring 1950). In the models, like the present one, which consider total relaxation of boundary shear stresses the numerical constant is about 50 % higher than in those calculations which assume a stress distribution typical of a homogeneous solid. The equation can be generalized further by inclusion of the Coble or grain boundary creep (Coble 1963) component by replacing the diffusion coefficient D with $(D+\pi D_g \delta/d)$, where D_g is the grain boundary diffusion coefficient and δ the boundary width.

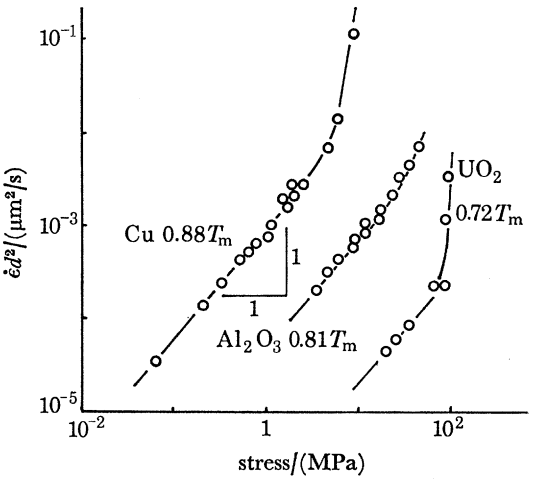

FIGURE 11. The observed linear dependence of creep rate with applied stress for three materials deforming in diffusion creep (Cu; Burton & Greenwood 1970; Al_2O_3: Davies & Sinha Ray 1972; UO_2: Poteat & Yust 1968).

The linear relation between creep rate and stress has been recently reviewed as well as the $1/d^2$ dependence for Nabarro–Herring creep and $1/d^3$ dependence for Coble creep (Burton 1977). Figure 11 shows creep data for Cu (Burton & Greenwood 1970), UO_2 (Poteat & Yust 1968) and Al_2O_3 (Davies & Sinha Ray 1972). The creep rate is compensated for grain size to allow for simultaneous grain growth during the test. The data show the linear relation between creep rate and uniaxial stress at low stresses. Increasing the stress rapidly increases the rate of dislocation creep, which is an independent process, and this eventually becomes the dominant deformation mechanism.

The value of the numerical constant in equation (11) is usually difficult to assess accurately from experimental data because of uncertainty in the diffusion coefficient. There are exceptions, and five independent observations of the volume self-diffusion coefficient in copper agree within a factor of 1.5 (Butrymowicz, Manning & Read 1974) giving an observed value from figure 11 of 18 with an upper and lower limit of 27 and 12 respectively. The agreement with theory is good considering the two dimensional nature and regularity of hexagonal grains.

The stress on the boundary calculated earlier was an average value for a particular boundary. When the grains deform by diffusion creep the vacancy flux leaving unit area of boundary is constant over the entire length of a particular boundary. The flux is proportional to the difference in normal tensile forces acting locally on source and sink and inversely proportional to the diffusion distance. Near a triple point the diffusion distance is small so the boundary stress is also small and tends to zero at the triple point. This also satisfies the requirement that

there is no instantaneous change in stress at the triple point. At the centre of the boundary the stress is largest reaching a value of 1.44 times the average value. This is illustrated in figure 12.

The distribution of stress is sensitive to the deformation mode of the grains. If for instance the dominant mechanism is dislocation creep, grain boundary sliding concentrates stress at the triple points, in complete contrast to diffusion creep. Figure 13, plate 2, illustrates this point in aluminium containing precipitates (Pond *et al.* 1976). The perpendicular grid lines superimposed on the surface before creep show signs of grain boundary shear between grains 1 and 3. The shear on this boundary has concentrated the stress at the triple point creating a slip band in the adjacent grain. High localized stresses can lead to triple point cracking. Alternatively if diffusion creep were rapid the stress concentrations would be absent, suppressing cracking.

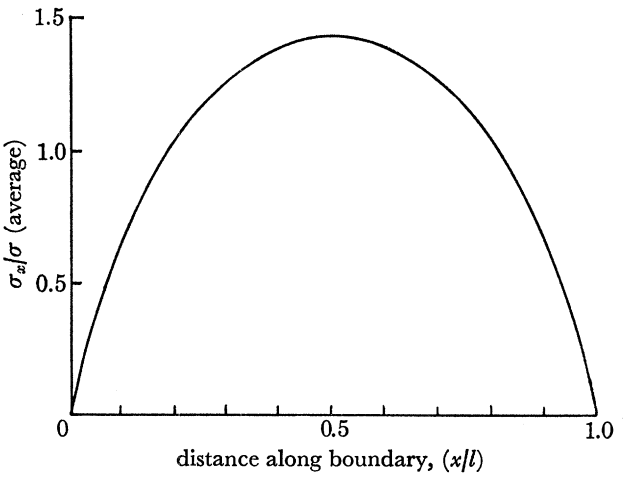

FIGURE 12. The variation of normal boundary force with distance along the boundary for a material deforming by Nabarro–Herring creep.

5. GRAIN BOUNDARIES AS SOURCES AND SINKS FOR VACANCIES

A second type of creep can occur in which the grain interior does not deform and in which shear forces play an important part in determining the grain trajectories. The application to physical situations is best understood by considering the operation of grain boundary vacancy sinks and sources. Several possible models are in existence and the mechanism of vacancy absorption on grain boundary dislocations is not completely clear, but situations where boundary shear stresses develop can often be envisaged.

Two types of boundary will be considered here, one in which vacancies are absorbed by dislocation (or a similar defect) climb in the boundary (McLean 1971; Gates 1973; Das & Marcinkowski 1972; Ashby 1969) and the second in which dislocation motion is unnecessary. The first is illustrated in figure 14 (*a*) in which just two sets of parallel dislocations with arbitrary Burgers vectors inhabit the boundary. If one set of dislocations is mobile and moves by simultaneous glide and climb the material on both sides of the boundary is displaced normally and sheared relative to the boundary plane. A vacancy flux is required which may have to come from another part of the crystal. Motion of the second set of dislocations can provide the vacancies enabling sliding to take place at a rate limited only by vacancy diffusion between

dislocations. If the material is deforming by diffusion creep the supply of vacancies from external sources is limited by diffusion across the grain. The much shorter diffusion path between dislocations enables sliding to rapidly release the boundary shear forces. In three dimensions three arbitrary sets of dislocations are required to enable independent boundary sliding in any direction. In general, three sets of intrinsic dislocations are necessary to provide coincidence when the lattices on either side of the boundary are at some random orientation.

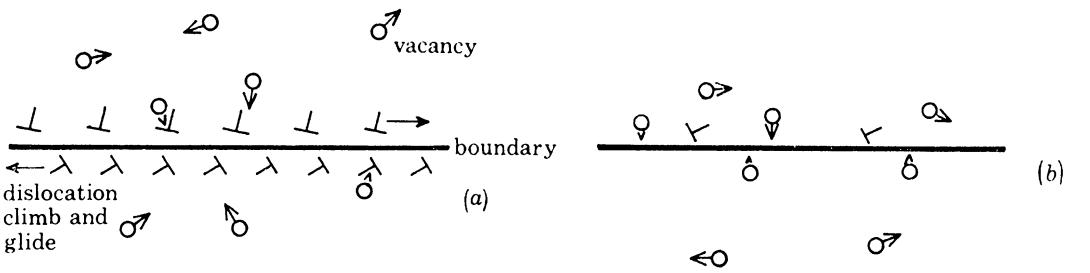

FIGURE 14. A schematic diagram of a grain boundary in which (*a*) vacancies condense on dislocation cores producing simultaneous glide and climb and (*b*) vacancy condensation is independent of the dislocation structure.

Several situations may develop which limit the mobility of boundary dislocations. Many materials exhibit a marked decrease of the diffusion creep rate when the stress is reduced to a value often in the range 1–10 MPa. The creep rate is then proportional to $(\sigma - \sigma_0)$, where σ_0 is the threshold stress.

This may result from a reduction in the extrinsic dislocation nucleation rate in the boundary (Burton 1973) or from precipitates blocking the path of boundary dislocations (Harris, Jones, Greenwood & Ward 1969). In both cases the inhibition of dislocation motion inhibits the ability of boundaries to emit vacancies and also prevents the dislocations from rapidly relaxing the shear forces. Diffusion creep rates are invariably slow near the threshold stress which limits the ultimate specimen strain. As a consequence morphological changes in grain structure are small and unlikely to be observed.

In direct contrast the strains realized in stage II superplastic creep are extremely large. Deformation takes place predominantly at the grain boundary and the grain interior often remains undeformed. Low stress stage II creep has the following attributes: (*a*) no evidence of internal slip lines; (*b*) scratch offsets are sharp; (*c*) an almost equiaxed structure; (*d*) grains relatively dislocation free; (*e*) grains rotate; (*f*) grains switch neighbours (see Edington, Melton & Cutler 1976). Several deformation mechanisms are based on grain boundary dislocations with motion limited by diffusion barriers in the grain boundary structure or grain boundary dislocation pileups near the triple point. In each case the mechanism limits the relaxation of both shear forces and normal boundary forces.

If boundary dislocation motion is unnecessary for vacancy emission or absorption the sliding mechanism will be completely independent of diffusion creep (figure 14*b*). If in this case the sliding process has a different activation energy or stress dependence from diffusion creep, situations can occur where sliding is rate controlling. Shear forces will develop on the boundaries but the normal forces will everywhere relax to some constant value dependent on the externally applied stress system.

6. Grain boundary sliding control of creep

Previously it was shown that shear forces are likely to develop on grain boundaries during diffusion creep at low stresses near a threshold stress and during stage II superplastic creep. The creep rate will be controlled either by the shear process with rapid relaxation of normal forces or by simultaneous slow relaxation of both normal and shear forces. In both cases the important feature from the point of grain motion is the effect of the shear forces. The friction which develops between grains leads to rotation of the grain. This is not to be confused with apparent rotation resulting from motion of the grain boundaries. The process to be discussed rotates the lattice whereas boundary migration leaves the lattice orientation unchanged. The principle of grain rotation is illustrated in figure 15 for square grains. The dotted lines (figure 15*a*) join the grain centres. When deformed uniaxially (figure 15*b*) material is redistributed between boundaries and the boundaries slide. When the boundary shear forces are not zero the externally applied forces do work sliding the boundaries.

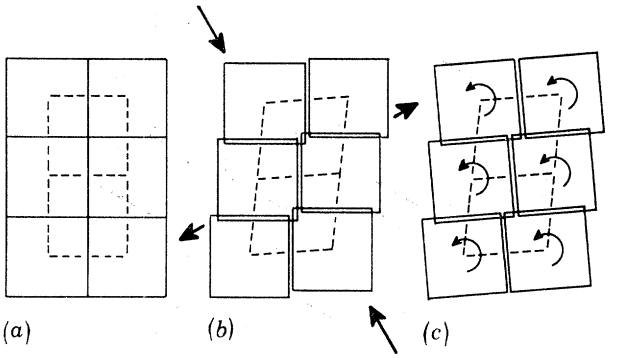

Figure 15. Six square grains (*a*) are deformed uniaxially, (*b*) producing grain boundary sliding on all faces. Grain rotation (*c*) allows reduction of the sliding displacement of the vertical faces without change in specimen strain.

In the example figure 15(*b*) the vertical and horizontal boundaries slide by equal amounts. The boundary viscosity, in general, will not be exactly uniform but can show variation due to a number of effects such as mis-orientation and precipitate density. If the vertical boundaries are more viscous than the horizontal boundaries, sliding can be reduced on the vertical boundaries by allowing the grains to rotate. In figure 15(*c*) sliding has been reduced to zero on the vertical boundaries while maintaining the same bulk or grain centre strain. In this way a given strain can be achieved with a smaller expenditure of energy.

The optimum rotation can be calculated by minimizing the rate of doing work during deformation. This is now done for regular hexagons. The same problem has been treated in three dimensions for a cubic array of grains (Beeré 1977). The results are very similar with the exception that when the boundaries are all equally resistant to sliding the cubic grains must still rotate by a small amount (see appendix).

The hexagonal array is illustrated in figure 16. The deformation of a grain is indistinguishable from its neighbours and again the three types of boundary are labelled a, b and c. (This analysis differs from the one previously where the grain deformation was allowed to vary between grains (Beeré 1976).)

The sliding displacement strain rate $\dot{x}_a$ on the 'a' boundaries is given by

$$\dot{x}_a = \dot{S}_a - \dot{\omega} d, \tag{12}$$

where $\dot{S}_a$ is the shear displacement rate at the grain centre. The sum of the grain centre shears is zero (equation (6)), hence the sum of the grain boundary shears is

$$\dot{x}_a + \dot{x}_b + \dot{x}_c = -3\dot{\omega} d. \tag{13}$$

From equations (12) and (13) the grain centre shear is

$$3\dot{S}_a = 2\dot{x}_a - \dot{x}_b - \dot{x}_c. \tag{14}$$

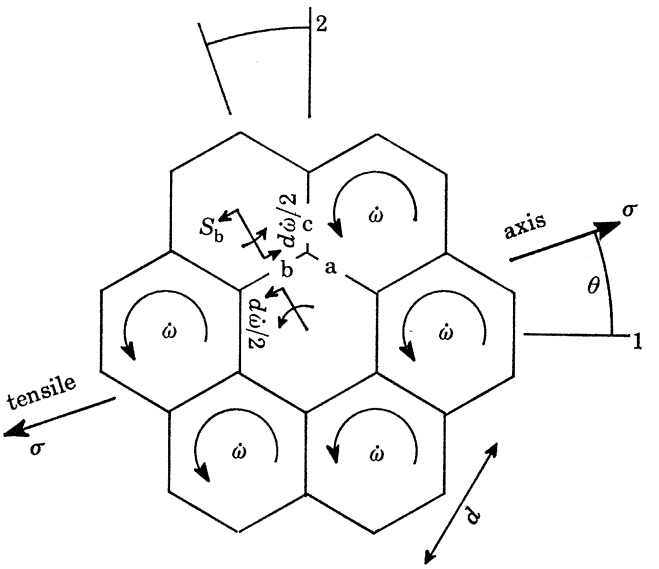

FIGURE 16. The system of grain rotations for hexagons.

Previously the bulk strain ϵ was found in terms of the grain centre shears (equation (9)). Substituting the grain boundary shears,

$$2\sqrt{3} d\dot{\epsilon} = (\dot{x}_a - \dot{x}_b)\,(4\cos^2\theta - 2) + (\dot{x}_a + \dot{x}_b - 2\dot{x}_c)\,(4\sin\theta\cos\theta/\sqrt{3}). \tag{15}$$

The creep rate may now be calculated if it is known how the shear rate varies with stress. When the normal and shear displacements on the boundary are interdependent processes the boundary shear rate will depend on both normal and shear stress. When normal and shear displacements are independent processes the normal stresses can be relaxed independently of the shear forces. In the following calculation it is assumed that the normal stresses assume their fully relaxed values (i.e. $\sigma_a = \sigma_b = \sigma_c$). This case is developed because the calculation is simplified, but the results are not likely to be greatly different for the case of a general system of normal stresses.

The shear rate will be given by an equation of the type

$$\dot{x}_a = \lambda_a |\tau_a^{n-1}|\,\tau_a, \tag{16}$$

where the modulus is to ensure the correct shear direction when n is even and λ depends on the material and creep mechanism

When the boundary shear rate varies linearly with stress ($n = 1$) and all boundaries are equally resistant to shear, the creep rate is given by

$$\dot{\epsilon} = \lambda\sigma/d, \tag{17}$$

independent of the orientation of the grains to the applied uniaxial stress, σ. When $n = 2$ the creep rate is given by

$$\dot{\epsilon} = \tfrac{1}{2}\sqrt{3}\,\lambda\sigma^2/d. \tag{18}$$

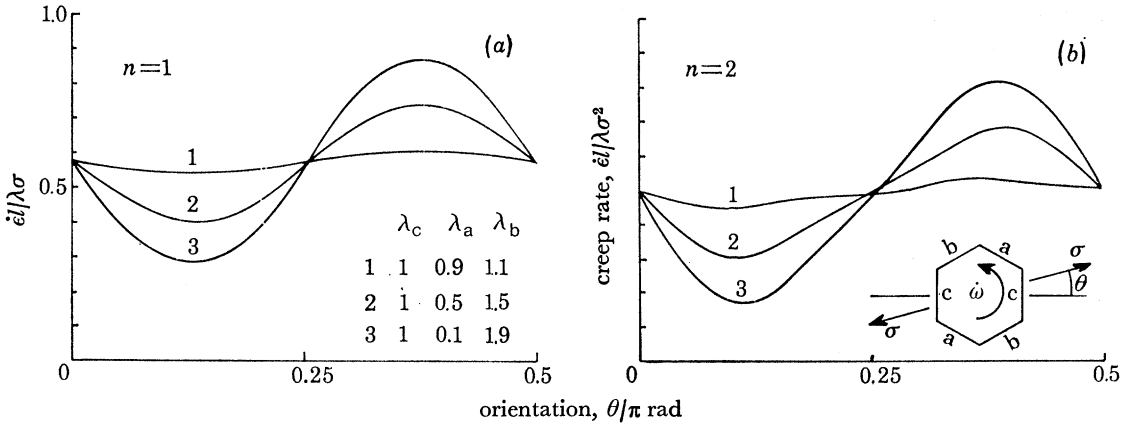

FIGURE 17. The variation of creep rate with orientation of the applied stress for grain boundary sliding control of creep when the sliding mechanism depends linearly on stress (*a*) and on stress squared (*b*). The numbers 1, 2 and 3 refer to variation in the anisotropy of sliding resistance.

If boundary viscosity varies with boundary orientation the creep rates have to be calculated numerically. This is done for stress exponents of $n = 1$ and $n = 2$ (figures 17*a* and *b* respectively). The average value of sliding resistance is kept constant, but a variation of up to a factor of ten is allowed between boundaries. The creep rate is dependent on orientation although the average creep rate for a random distribution of orientations is unchanged.

The optimum rate of grain rotation is found by minimizing the work done in achieving a fixed strain. This is readily found provided that the normal forces are relaxed, that is if the work done by the externally applied stress is primarily spent in grain boundary sliding. The rate of working on unit area of boundary is then the product of shear velocity and shear stress

$$W \propto \dot{x}_a\tau_a + \dot{x}_b\tau_b + \dot{x}_c\tau_c;$$

written in terms of the sliding shears, this becomes

$$W \propto (1/\lambda_\alpha)^{1/n}\,|\dot{x}_\alpha|^{(1+n)/n} \quad (\alpha = \mathrm{a, b, c}),$$

and in terms of grain centre motion and rotations

$$W \propto (1/\lambda_\alpha)^{1/n}\,|\dot{S}_\alpha - \dot{\omega}d|^{(1+n)/n} \quad (\alpha = \mathrm{a, b, c}).$$

The optimum rate of rotation is found by minimizing the rate of work done, W, at constant specimen strain rates, $\dot{S}_a$, $\dot{S}_b$ and $\dot{S}_c$.

Putting $\partial W/\partial\dot{\omega} = 0$ and solving numerically gives the results illustrated in figure 18 (*a*, *b*) for $n = 1, 2$, respectively. The resistance to sliding, λ, is varied by up to a factor of 10 to 1 with orientation. As expected, increasing the anisotropy of the grains increases the rotation.

The calculations can be compared with observed rotations in the scanning electron microscope (Geckinli & Barrett 1976). Differentiating the variation of angle with strain (figure 3)

gives the strain rate compensated rate of rotation, $\dot{\omega}/\dot{\epsilon}$, which is shown in figure 19. The maximum observed rate of rotation is about $0.6\dot{\epsilon}$. This rate would be achieved in the present model when the boundaries vary by an order of magnitude in viscosity.

Although quite high rates of rotation are momentarily achieved the maximum angular rotation is seldom more than 30° (figure 3). The grains appear to oscillate about a mean orientation. This behaviour is predicted by the present model. If the angular rotation, $\dot{\omega}$, is positive (figure 18*b*), then the rate of change of the angle θ is negative. This implies that a grain situated on curve 3 in figure 18 (*b*) will tend to move to the position of stable equilibrium where $\dot{\omega} = 0$ on the left hand side of the diagram.

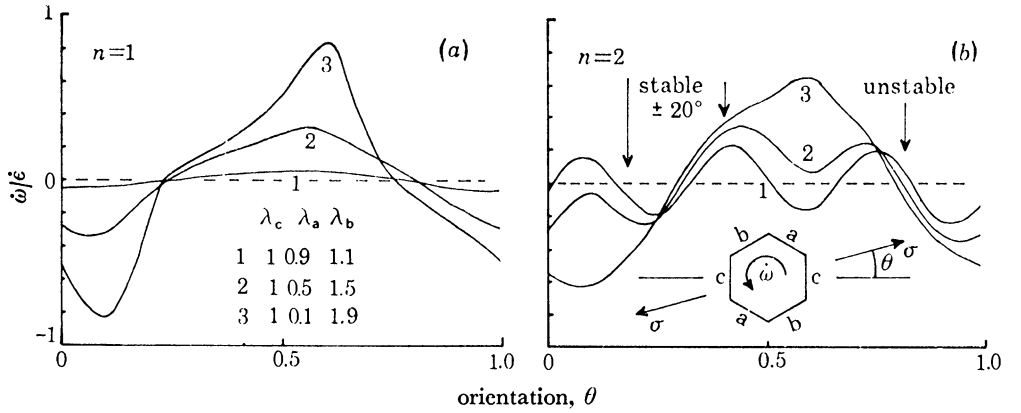

FIGURE 18. The rates of grain rotation for hexagons with anisotropic sliding resistance. The stable orientation is shown in (*b*).

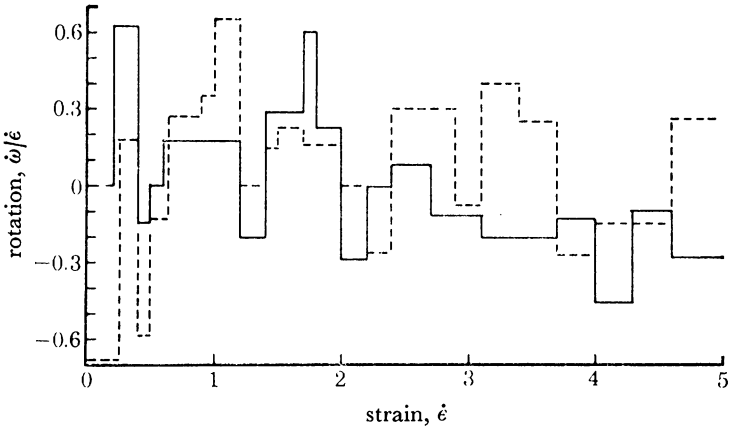

FIGURE 19. The observed rate of grain rotation calculated from figure 3.

In this example the 'a' boundary is the most viscous by an order of magnitude. The position of stability, $\dot{\omega} = 0$, is achieved when the 'a' boundary is perpendicular to the applied stress. Little sliding then takes place on this boundary and intuitively we have the correct result.

The stable configuration is disturbed by grain rearrangement during creep. Grain boundaries are often mobile and migrate during deformation resulting in simultaneous grain growth. Relative movement of the grain centres during deformation also requires grain boundary migration to maintain equilibrium angles at grain edges. This is illustrated in

figure 20 in which hexagons undergo a shear strain of 0.25. The boundaries have been constructed such that they always meet at angles of $\frac{2}{3}\pi$ at the triple point and pass midway between grain centres. The latter maintains a constant number of indistinguishable grains. In practice, limits on boundary mobility restrict the approach to ideal configurations. The important feature, though, is the rotation of the boundary.

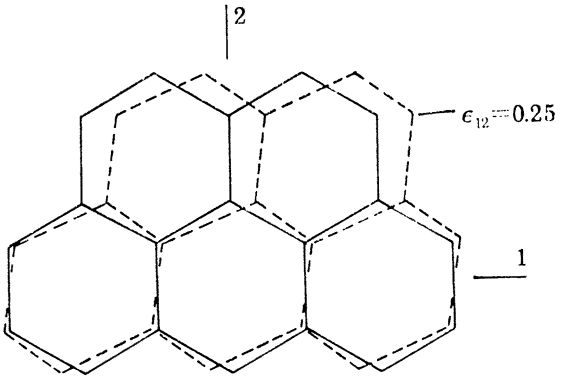

FIGURE 20. Regular hexagons deformed in shear. The position of the boundaries has been calculated assuming a constant number of identical grains maintaining equal angles at the triple points.

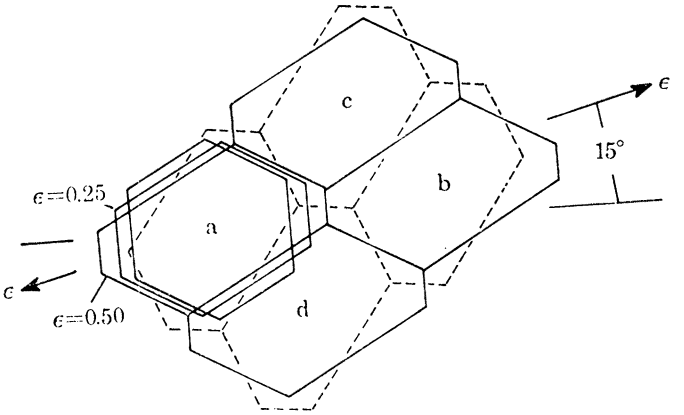

FIGURE 21. As figure 20, but deformed uniaxially. The broken lines show neighbour exchange maintaining a more equiaxed grain shape.

In contrast, figure 21 shows the same hexagonal configuration subjected to uniaxial strains of 0.25 and 0.50. Here the ideal configuration shows no boundary rotation. At 50 % strain the grains can reduce their boundary surface area (length) by neighbour exchange (Rachinger 1952; Ashby & Verrall 1973). This now results in boundary rotation.

In three dimensions boundary migration is complicated by the appearance of new grains at a surface. Also boundary sliding viscosity will vary with change in boundary angle even when adjacent lattices are kept at the same misorientation. Allowing for this grain rotation will still orientate normally to the stress axis those boundaries most resistant to sliding. Grain rearrangement will disturb these configurations, but equilibrium will be restored by rapid grain rotation.

7. Summary

Non-uniform deformation resulting from grain boundary sliding can be divided into three categories, namely (*a*) rigid grain interior with zero shear forces on boundary; (*b*) rigid grain interior with non-zero shear forces on boundary; (*c*) plastic deformation within grain. The first type, situation (*a*), is the classical picture of diffusion creep. Deformation is limited by the rate of vacancy diffusion across grains while the accommodating grain boundary sliding independently relaxes the shear forces. The second type of deformation (*b*) occurs when an interface reaction limits the deformation rate. The interface kinetics result from the nature of defects in the grain boundary. The friction which develops between the grains during grain boundary sliding causes the lattice of the grain to rotate. The fields of application are in diffusion creep near a threshold stress and superplastic creep. Lastly, the grain interiors deform plastically by dislocation creep when the applied stress is sufficiently large.

This paper is published by permission of the Central Electricity Generating Board.

Appendix

Figure A 1 shows one cube of an array located in a tensile specimen at some random orientation to the tensile axis. The interior of the grain is considered to be rigid with all deformation taking place at or near the grain boundary. Shear displacement between adjacent grain centres takes place by shear on the boundary. If the rate of grain boundary sliding is independent of the normal stress across the boundary (sliding an independent process) the shear rate is related to the boundary shear stress by a relation of the type $\dot{\epsilon} = \lambda\sigma^n/d$, where λ depends on the boundary viscosity, d is the cube edge length and n is the stress exponent.

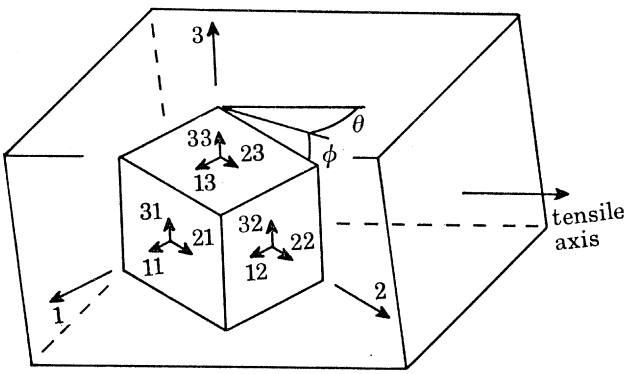

Figure A 1. A cube randomly orientated in a tensile specimen.

If σ_{31} and σ_{21} are the shear stresses on face 1 (figure A 2*b*), then the shear in the 2 direction is given by

$$\dot{\epsilon}^{s}_{21} = (\lambda/d)\,(\sigma^2_{31}+\sigma^2_{21})^{(n-1)/2}\,\sigma_{21}, \qquad \text{(A 1)}$$

where the superscript s denotes sliding and $(d\dot{\epsilon}^{s}_{21})$ is the actual displacement on the face. In the absence of grain rotation $\dot{\epsilon}^{s}_{21}$ is equal to $\dot{\epsilon}_{21}$, the shear strain between grain centres. An equiaxed

polycrystal does not undergo rotation when stretched uniaxially and so $\dot{\epsilon}_{21} = \dot{\epsilon}_{12}$. From equation (A 1) and the similar expression for $\dot{\epsilon}^{s}_{12}$ it follows that

$$(\sigma^2_{31} + \sigma^2_{21})^{(n-1)/2}\, \sigma_{21} = (\sigma^2_{12} + \sigma^2_{32})^{(n-1)/2}\, \sigma_{12}, \tag{A 2}$$

but $\sigma_{12} = \sigma_{21}$ and so from equation (A 2)

$$\sigma_{31} = \sigma_{32} \quad (n \neq 1). \tag{A 3}$$

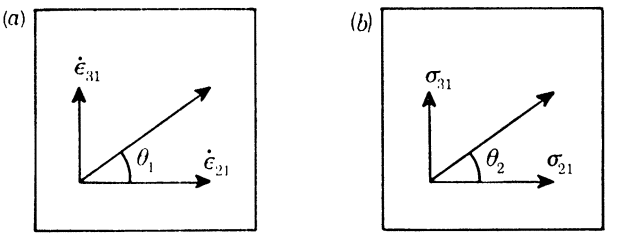

FIGURE A 2. The shear displacement and shear stress on face 1 of the cube.

Equating the other shear strains in the same manner it is found that all the shear stresses must be equal. This absurdity is removed when the grains are allowed to rotate at rates $\dot{\omega}_1$, $\dot{\omega}_2$ and $\dot{\omega}_3$ about the 1, 2 and 3 axis respectively (figure A 3). The rate of sliding on a face then depends on the grain centre shear and the rate of rotation. For instance the sliding displacement rate in the 1 direction on face 2 is given by

$$\dot{\epsilon}^{s}_{12} = \dot{\epsilon}_{12} - \dot{\omega}_3. \tag{A 4}$$

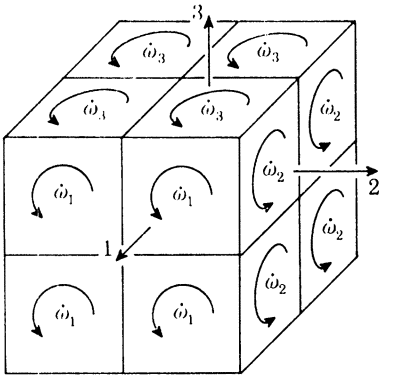

FIGURE A 3. The system of cube rotations.

When the array deforms by a given strain the cubes rotate by an amount which minimizes the energy dissipation required to achieve that strain.

If W_1 is the rate of working on face 1 then

$$W_1 \propto [(\dot{\epsilon}^{s}_{31})^2 + (\dot{\epsilon}^{s}_{21})^2]^{\frac{1}{2}} [\sigma^2_{31} + \sigma^2_{21}]^{\frac{1}{2}}, \tag{A 5}$$

or in terms of strains and rotations

$$\left.\begin{aligned} W_1 &\propto [(\dot{\epsilon}_{31} + \dot{\omega}_2)^2 + (\dot{\epsilon}_{21} - \dot{\omega}_3)^2]^{(1+n)/2n}; \\ W_2 &\propto [(\dot{\epsilon}_{12} + \dot{\omega}_3)^2 + (\dot{\epsilon}_{32} - \dot{\omega}_1)^2]^{(1+n)/2n}; \\ W_3 &\propto [(\dot{\epsilon}_{13} - \dot{\omega}_2)^2 + (\dot{\epsilon}_{23} + \dot{\omega}_1)^2]^{(1+n)/2n}, \end{aligned}\right\} \tag{A 6}$$

where W_2 and W_3 are the rates of working or faces 2 and 3 respectively. The total rate of energy dissipation is given by $W = W_1 + W_2 + W_3$ and the most favourable rotations are found by partially differentiating with respect to the rotations at constant cube centre strain rate, i.e. $\partial W/\partial\dot{\omega}_1 = \partial W/\partial\dot{\omega}_2 = \partial W/\partial\dot{\omega}_3 = 0$. The derivative with respect to $\dot{\omega}_1$ is

$$\partial W/\partial\dot{\omega}_1 \propto [(\dot{\epsilon}_{13} - \dot{\omega}_2)^2 + (\dot{\epsilon}_{23} + \dot{\omega}_1)^2]^{(1-n)/2n} (\dot{\epsilon}_{23} + \dot{\omega}_1) - [(\dot{\epsilon}_{12} + \dot{\omega}_3)^2 + (\dot{\epsilon}_{32} - \dot{\omega}_1)^2]^{(1-n)/2n} (\dot{\epsilon}_{32} - \dot{\omega}_1). \quad \text{(A 7)}$$

Next the shear stresses are written in terms of the strain rates. Since the shear stresses are related to sliding strains by an equation of the type $\sigma = (\dot{\epsilon}^s d/\lambda)^{1/n}$, σ_{23} is given by

$$\sigma_{23} = (d/\lambda)^{1/n} [(\dot{\epsilon}^s_{23})^2 + (\dot{\epsilon}^s_{13})^2]^{(1-n)/2n} \dot{\epsilon}^s_{23}, \quad \text{(A 8)}$$

or, in terms of grain centre strains and rotations,

$$\sigma_{23} = (d/\lambda)^{1/n} [(\dot{\epsilon}_{13} - \dot{\omega}_2)^2 + (\dot{\epsilon}_{23} + \dot{\omega}_1)^2]^{(1-n)/2n} (\epsilon_{23} + \dot{\omega}_1), \quad \text{(A 9)}$$

and similarly for σ_{32},

$$\sigma_{32} = (d/\lambda)^{1/n} [(\dot{\epsilon}_{12} + \dot{\omega}_3)^2 + (\dot{\epsilon}_{32} - \dot{\omega}_1)^2]^{(1-n)/2n} (\dot{\epsilon}_{32} - \dot{\omega}_1). \quad \text{(A 10)}$$

Reference to equations (A 7), (A 9) and (A 10) shows that putting $\sigma_{23} = \sigma_{32}$ implies that $\partial W/\partial\dot{\omega}_1 = 0$. Identically when $\sigma_{12} = \sigma_{21}$, $\partial W/\partial\omega_3 = 0$ and when $\sigma_{13} = \sigma_{31}$, $\partial W/\partial\omega_2 = 0$. Thus, when the cubes deform they follow the path of least energy expenditure which simultaneously satisfies the balance of shear stresses on the cube faces.

The cubes were considered to be equally resistant to sliding on all faces. If, however, sliding is easier say on face 1 than face 2 the material parameter λ takes on different values λ_1, λ_2 and λ_3 for faces 1, 2 and 3 respectively. If the above arguments are repeated with the new values of sliding resistance the same conclusions are reached.

The rotations and strain rates calculated for the cube model are in substantial agreement with the rates calculated for the hexagon model.

References (Beeré)

Ashby, M. F. 1969 *Scr. met.* **3**, 837.
Ashby, M. F. & Verrall, R. A. 1973 *Acta metall.* **21**, 149.
Beeré, W. 1976 *Met. Sci.* **10**, 133.
Beeré, W. 1977 (To be published.)
Bell, R. L. & Langdon, T. G. 1969 *Interfaces Conference* (ed. R. C. Gifkins), p. 115. Sydney: Butterworths.
Burton, B. 1973 *Met. Sci. J.* **11**, 337.
Burton, B. 1977 *Diffusion creep of polycrystalline materials*. Switzerland: Trans. Tech. Pub.
Burton, B. & Greenwood, G. W. 1970 *Acta metall.* **18**, 1237.
Butrymowicz, D. B., Manning, J. R. & Read, M. E. 1974 *J. phys. Chem., Ref. Data* **2**, 643.
Coble, R. L. 1963 *J. appl. Phys.* **34**, 1679.
Crossman, F. W. & Ashby, M. F. 1975 *Acta metall.* **23**, 425.
Das, E. S. P. & Marcinkowski, M. J. 1972 *Acta metall.* **20**, 199.
Davies, C. K. L. & Sinha Ray, S. K. 1972 *Spec. Ceram.* **5**, 193.
Edington, J. W., Melton, K. N. & Cutler, C. P. 1976 *Prog. mater. Sci.* **21**, 61.
Gates, R. S. 1973 *Acta metall.* **21**, 855.
Gates, R. S. 1975 *Phil. Mag.* **31**, 367.
Geckinli, A. E. & Barrett, C. R. 1976 *J. mater. Sci.* **11**, 510.
Gibbs, G. B. 1965 *Mém. Sci. Rev. Mét.* **62**, 781.
Harris, J. E., Jones, R. B., Greenwood, G. W. & Ward, M. J. 1969 *J. Aust. Inst. Met.* **14**, 154.
Herring, C. 1950 *J. appl. Phys.* **20**, 437.

PHILOSOPHICAL TRANSACTIONS OF THE ROYAL SOCIETY A MATHEMATICAL, PHYSICAL & ENGINEERING SCIENCES

Lifshitz, L. M. 1963 *Sov. Phys. J.E.T.P.* **17**, 909.
McLean, D. 1971 *Phil. Mag.* **23**, 182.
Pond, R. C., Smith, D. A. & Southerden, P. W. J. 1976 *4th Int. Conf. Strength Metals and Alloys*. Nancy, p. 378.
Poteat, L. E. & Yust, C. S. 1968 *Ceramic microstructures* (eds R. M. Zulraith & J. A. Pask). New York: Wiley.
Rachinger, W. A. 1952–3 *J. Inst. Met.* **81**, 33.
Raj, R. & Ashby, M. F. 1971 *Metall. Trans.* **2**, 1113.
Reynolds, G. L. 1977 Private communication.
Reynolds, G. L., Burton, B. & Speight, M. V. 1975 *Acta metall.* **23**, 573.
Speight, M. V. 1976 *Acta metall.* **24**, 725.
Stephens, R. N. 1971 *Phil. Mag.* **23**, 265.

Discussion

E. H. Rutter (*Geology Department, Imperial College, London, SW7*). Dr Beeré has shown that oscillatory grain rotations occur during diffusion creep of polycrystalline aggregates loaded along an irrotational finite strain path. In natural rock deformation a situation of particular interest is that of simple shear within a narrow zone (shear zone). In mylonite belts associated with major overthrusts, rocks may have suffered shear displacements in excess of *ca.* 1 km over shear zone widths often less than 100 m. A common microstructure involves early, severely flattened grains either partly or totally replaced by an aggregate of small (*ca.* 30 μm) recrystallized grains (White 1976), recrystallization being concentrated at old grain boundaries. One is tempted to wonder if this microstructure is stable over large ranges in strain because the new, small grains 'roll' over one another, the potential for dilation being counteracted by diffusion. A simple shear deformation involves a vorticity, so one might expect a bias in the sense of grain rotations which accompany grain boundary sliding. Does Dr Beeré know of observational data on any materials which indicate that such a rolling process occurs in high temperature creep during a vortical strain history?

Reference

White, S. H. 1976 The effects of strain on the microstructures, fabrics and deformation mechanisms in quartzites. *Phil. Trans. R. Soc. Lond.* A **283**, 69–86.

W. Beeré. The treatment of grain boundary sliding was confined to uniaxial tension but the principles can easily be applied to a shear deformation. Considering a two dimensional square array of grains by viewing the cubic grains, figures A 1, A 2 and A 3, along the 1 axis, the shear strain rates between cube centres $\dot{\epsilon}_{23}$ and $\dot{\epsilon}_{32}$ are given by:

$$\dot{\epsilon}_{23} = \dot{\epsilon}^{s}_{23} - \dot{\omega}_1;$$
$$\dot{\epsilon}_{32} = \dot{\epsilon}^{s}_{32} + \dot{\omega}_1,$$

where $\dot{\epsilon}^{s}_{23}$ is the surface sliding velocity on a unit square and $\dot{\omega}_1$ is the angular velocity. Subtraction gives the latter:

$$\dot{\omega}_1 = \tfrac{1}{2}(\dot{\epsilon}_{32} - \dot{\epsilon}_{23}) + \tfrac{1}{2}(\dot{\epsilon}^{s}_{23} - \dot{\epsilon}^{s}_{32}).$$

The sliding rates $\dot{\epsilon}^{s}_{23}$ and $\dot{\epsilon}^{s}_{32}$ depend on the boundary viscosity. If for instance $\dot{\epsilon}^{s}_{23} = \lambda_3 \sigma^{n}_{23}$ where λ_3 depends on the boundary properties and n is the stress exponent, then since $\sigma_{23} = \sigma_{32}$, the angular velocity is given by

$$\dot{\omega}_1 = \tfrac{1}{2}(\dot{\epsilon}_{32} - \dot{\epsilon}_{23}) + \tfrac{1}{2}\sigma^{n}_{23}(\lambda_3 - \lambda_2).$$

Clearly if the boundaries are all equally resistant to sliding, $(\lambda_3 - \lambda_2)$ is zero and the angular velocity $\dot{\omega}_1$ is identical to the bulk macroscopic rotation.

Rotation of a grain relative to the macroscopic axes requires differences in sliding resistance on different faces of a grain. Two phase superplastic materials consisting of α and β grains contain α–α, α–β and β–β boundaries. An α grain will have α–α and α–β boundaries which can account for the differences in sliding resistance. Superplastic alloys are usually deformed in tension. The mechanism proposed for grain rolling operates equally in both tension and torsion.

PHILOSOPHICAL TRANSACTIONS OF THE ROYAL SOCIETY A MATHEMATICAL, PHYSICAL & ENGINEERING SCIENCES

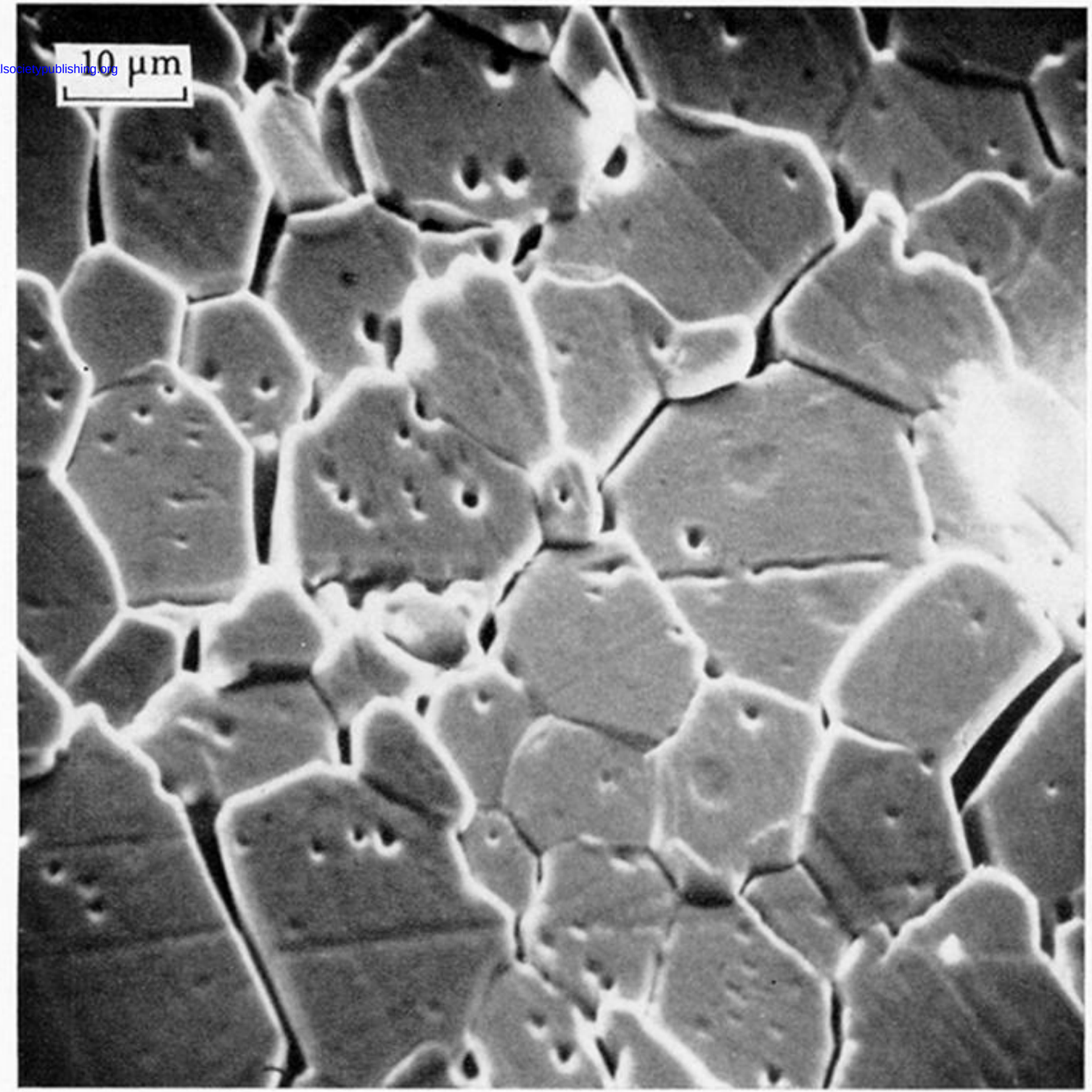

FIGURE 2. A scanning electron micrograph of UO_2. The initially flat polished surface shows ledges, sliding offsets of surface scratches and cracks resulting from grain boundary sliding during creep. (Reynolds *et al.* 1975.)

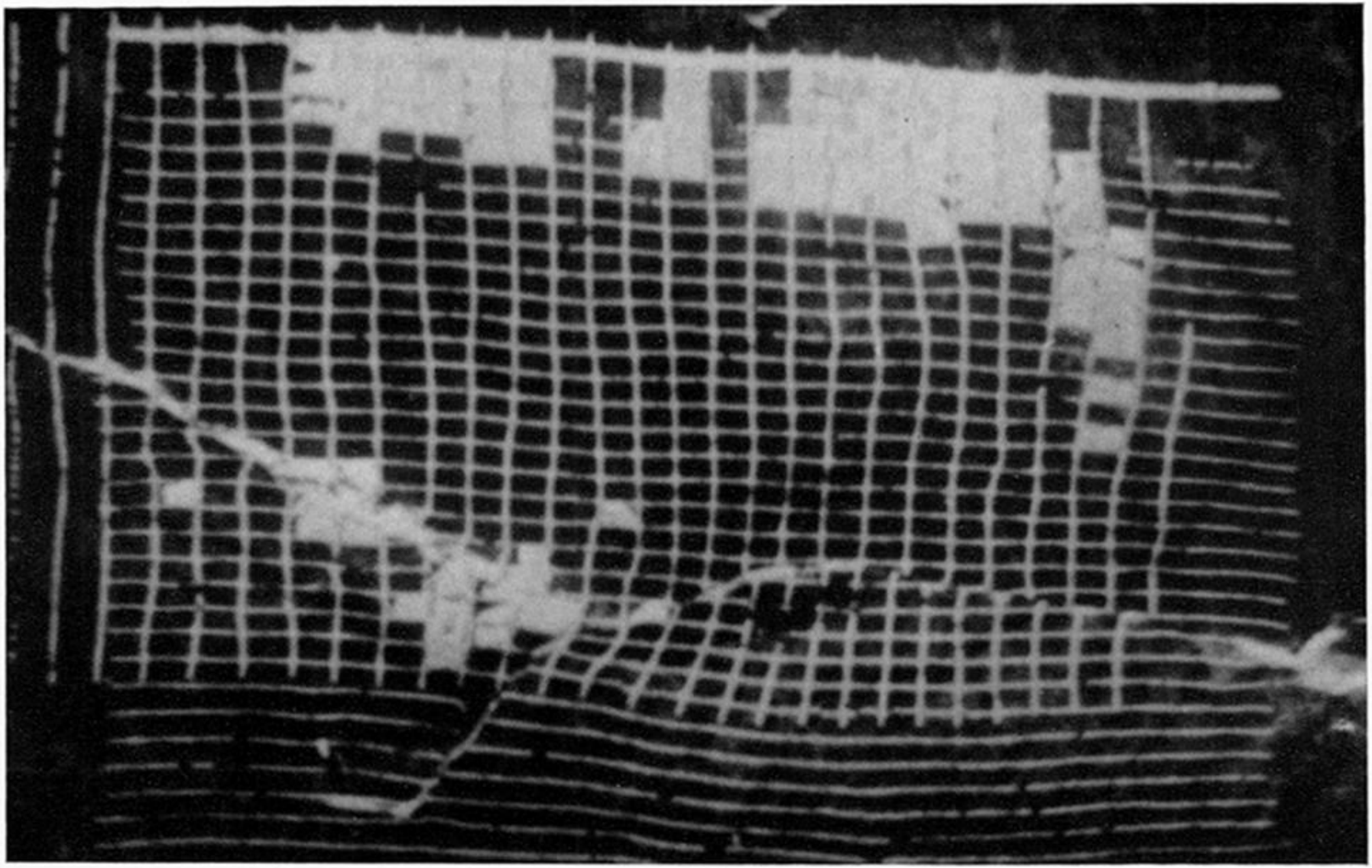

FIGURE 4. Deformation by grain boundary sliding and dislocation creep of an initially rectangular 8 μm grid on aluminium. (Pond *et al.* 1976.)

PHILOSOPHICAL TRANSACTIONS OF THE ROYAL SOCIETY A MATHEMATICAL, PHYSICAL & ENGINEERING SCIENCES

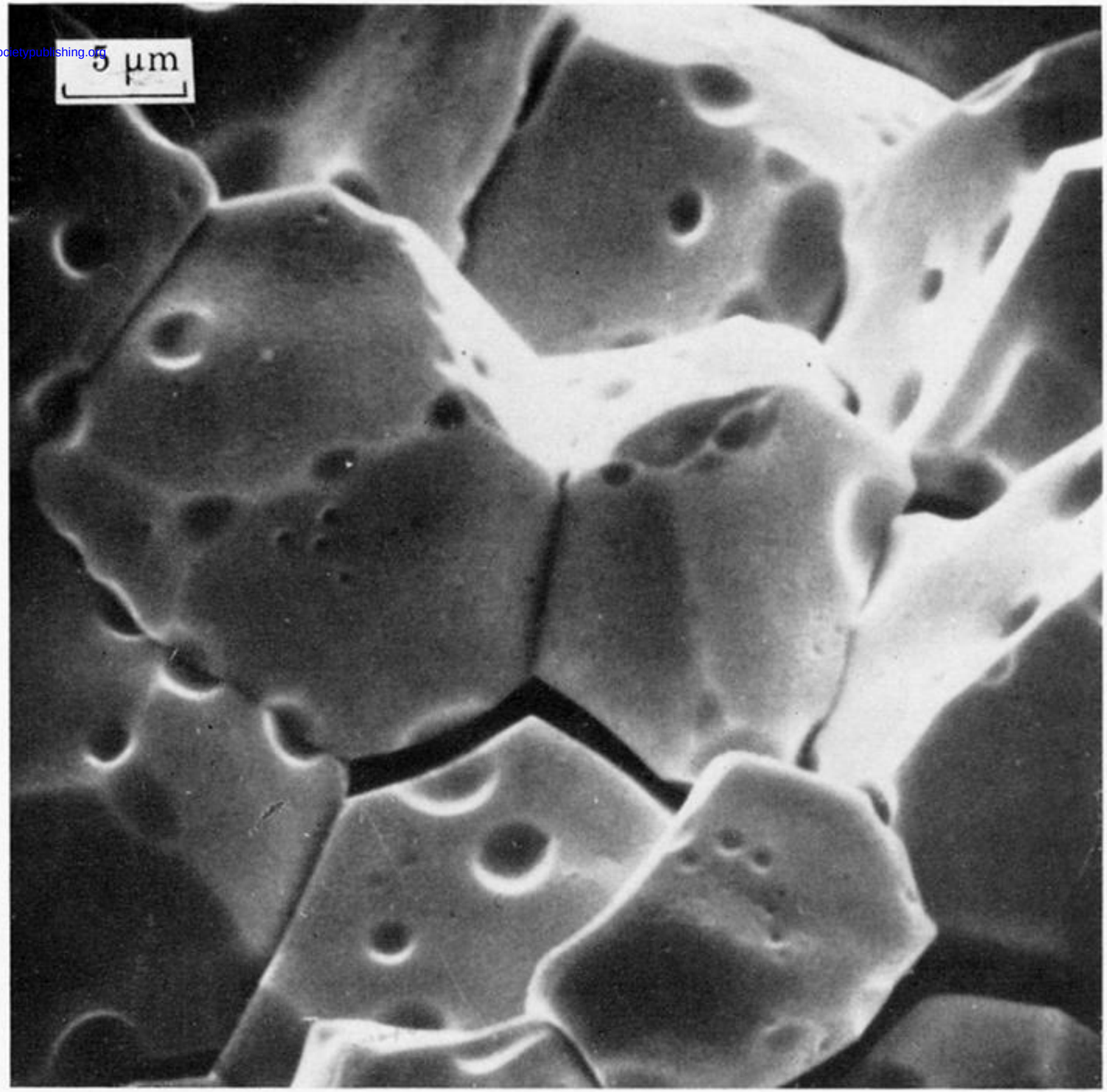

FIGURE 8. Cracks in a UO_2 compression specimen. The wedging action of adjacent grains coupled with grain boundary sliding produces tensile forces and cracking. (Reynolds *et al.* 1975.)

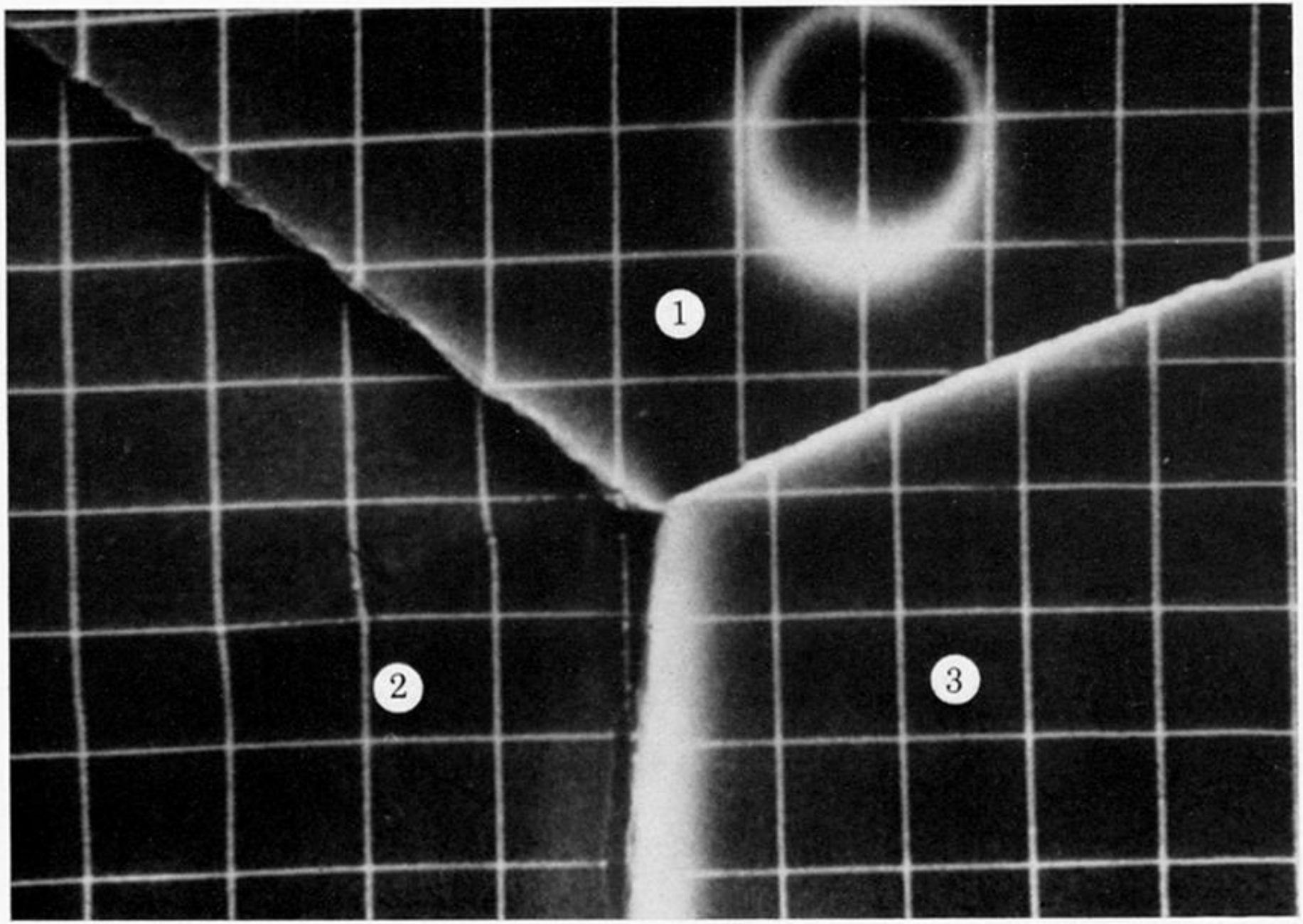

FIGURE 13. Grain boundary sliding in aluminium revealed by displacements in an initially rectangular 8μm grid. Sliding between grains 1 and 3 has created a slip band in grain 2. (Pond *et al.* 1976.)